INTERNATIONAL JOURNAL OF GEOMAGNETISM AND AERONOMY
VOL. 4, NO. 1, PAGES 47–55, APRIL 2003

Model results for the midlatitude daytime E region: EUV ionization rate and $\alpha(NO^+)$ relationship

A. V. Mikhailov

Institute of Terrestrial Magnetism, Ionosphere and Radio Wave Propagation, Troitsk, Russia

Abstract. The problem with low calculated N_mE for midlatitude daytime E layer is discussed using Millstone Hill winter $N_e(h)$ observations compared with model calculations. A proposal to obtain the observed N_mE values due to an increase in the 50–100 Å flux increase should be ruled out as this distorts the proportion between UV and X-ray contributions to the total photoionization rate of the E region in favor of X ray and leads to a contradiction in the N_mE observations during solar flares. The Extreme Ultraviolet (EUV) model by *Nusinov* [1992] provides a proper proportion between UV and X-ray contributions while the Extreme Ultraviolet Model for Aeronomic Calculations (EUVAC) does not. A reduction of $\alpha(NO^+)$, by taking into account $T_e > T_n$ in the E region as it follows from probe measurements, may be considered as a plausible solution, although such probe results are not confirmed by incoherent scatter observations. The E-layer ion composition with $[NO^+] > [O_2^+]$ corresponding to rocket observations may be obtained in model simulations by using an appropriate [NO] height distribution.

1. Introduction

Midlatitude ionospheric E layer has been studied for many years, nevertheless there are still problems with its description. While available empirical N_mE models like International Reference Ionosphere (IRI) [*Bilitza*, 1990] reproduce regular N_mE variations with sufficient accuracy, a theoretical approach based on current EUV solar flux models and commonly accepted dissociative recombination rate constants for NO^+ and O_2^+ ions usually underestimates N_mE by 30–40% [*Buonsanto et al.,* 1995; *Titheridge*, 1997]. Because of the square-law loss process this 40% deficit in N_mE implies a 100% increase in the ionization rate at the E-layer peak (105–110 km). Some approaches have been proposed to overcome this problem. *Ivanov-Kholodny and Nusinov* [1979] used low $\alpha(NO^+)$ value by *Mul and McGowan* [1979] along with strong seasonal variations in the $[O_2]$ scale height in the 100–110 km height range. *Antonova et al.* [1996] took into account vibrationally excited NO^+ and O_2^+ ions, and this allowed them to explain N_mE and h_mE seasonal variations. *Titheridge* [1996, 1997], using a full allowance for secondary ionization with EUV radiations down to 25 Å and a 33% additional increase in the radiation with $\lambda < 150$ Å in the Extreme Ultraviolet Model for Aeronomic Calculations (EUVAC)[*Richards et al.,* 1994], could describe the observed N_mE values. Although there is large uncertainty in EUV fluxes in this spectrum range, such an increase of the EUV flux in the 50–150 Å range seems unjustified, as is shown below. The fluxes in this spectrum range have already been tripled in the EUVAC model [*Richards et al.,* 1994] compared to the reference spectrum F74113 measured on 23 April 1974 ($F_{10.7} = 74$), and this factor is kept in the model for all levels of solar activity.

Calculated NO^+/O_2^+ ratio is another problem in the E-region theoretical modeling [*Buonsanto et al.,* 1995; *Titheridge*, 1997]. Usually, the calculated NO^+/O_2^+ ratio is less, compared to rocket observations in the E region [*Danilov*, 1994; *Danilov and Semenov*, 1978; *Danilov and Smirnova,* 1995, and references therein]. *Buonsanto et al.* [1995] and *Titheridge* [1997], analyzing this problem, suggested that our understanding of the NO^+ chemistry may be incomplete.

Paper number GAI00345.
CCC: 1524–4423/2003/0401–0345$18.00

The online version of this paper was published 14 January 2003.
URL: http://ijga.agu.org/v04/gai00345/gai00345.htm
Print companion issued April 2003.

Table 1. Comparison of Nusinov and EUVAC Models for Solar Minimum and Maximum Conditions

λ, Å	Nusinov $F_{10.7}$=74	EUVAC F74113	Nusinov $F_{10.7}=200$	EUVAC $P=200$
50–100	0.415	1.200	1.167	2.642
100–150	0.507	0.450	0.949	0.835
150–200	6.722	4.800	11.464	12.504
200–250	6.219	3.100	13.459	10.335
256	0.616	0.460	0.984	0.613
284	0.856	0.210	4.424	3.680
250–300	2.829	1.679	9.694	7.012
304	10.054	7.700	16.686	12.860
300–350	1.658	0.965	5.490	3.565
368	0.916	0.650	1.424	1.164
350–400	0.626	0.314	1.966	1.691
400–450	0.571	0.383	1.257	0.723
465	0.413	0.290	0.674	0.551
450–500	0.874	0.285	2.157	0.977
500–550	0.747	0.452	1.416	0.927
554	0.926	0.720	1.368	1.002
584	1.987	1.270	3.841	2.056
550–600	0.537	0.353	0.952	0.514
610	0.992	0.530	2.118	1.559
630	2.170	1.590	3.570	2.224
600–650	0.533	0.342	1.161	0.826
650–700	0.286	0.230	0.504	0.348
703	0.487	0.360	0.698	0.491
700–750	0.222	0.141	0.428	0.221
765	0.254	0.170	0.419	0.249
770	0.378	0.260	0.936	0.660
789	0.963	0.702	1.411	0.978
750–800	1.056	0.758	2.118	1.192
800–850	2.426	1.625	4.360	2.564
850–900	5.876	3.537	11.068	5.946
900–950	4.637	3.000	8.805	4.794
977	6.251	4.400	9.568	6.481
950–1000	1.998	1.475	3.627	2.257
1026	5.730	3.500	10.857	5.677
1032	2.988	2.100	5.313	3.431
1000–1050	2.947	2.467	5.361	3.762
Total	77.7	52.5	151.8	107.3

Fluxes are given in 10^9 ph cm^{-2} s^{-1} units.

The aim of the paper is to compare E-region simulations with the Millstone Hill $N_e(h)$ observations given by *Buonsanto et al.* [1995] and to draw a conclusion on EUV model fluxes and $\alpha(\mathrm{NO}^+)$ dissociative recombination rate coefficient needed to obtain the observed N_mE for different levels of solar activity. A possible way to obtain NO concentrations, providing the observed $\mathrm{NO}^+/\mathrm{O}_2^+$ ratio in model International Reference Ionosphere calculations, is proposed as well.

2. Ionospheric Model

Midlatitude regular ionospheric E layer is known to be controlled by photochemical processes. A two-component model by Nusinov [*Bruevich and Nusinov*, 1984; *Nusinov*, 1984, 1992] with further corrections by *Nusinov et al.* [1999] is used to calculate EUV fluxes in 48 wavelength intervals with $8 \leq \lambda \leq 1050$ Å. The intensity of the EUV fluxes in this model depends on slowly varying F_{bg} emission at 10.7 cm wavelength and on radio emission from active areas on the Sun, $F_{10.7}$ [*Nusinov*, 1984]. The background F_{bg} emission varies from $F_{\mathrm{bg}} = 60 - 65$ (in 10^{-22} W m^{-2} Hz^{-1}) at solar minimum to $F_{\mathrm{bg}} \approx 120$ at solar maximum. The X range ($\lambda < 100$ Å) includes 13 wavelength bins. Ionization by a strong Lyman-α line ($\lambda = 1216$ Å) is taken into account according to the *Katjushina et al.* [1991] model. Although this emission gives only around 1% of the total ionization rate at the E-layer peak, it becomes important at lower heights. For further discussion, Table 1 gives fluxes according to the Nusinov and EUVAC models in the same wavelength bins as used in the EUVAC model. Solar minimum of 23 April 1974 ($F_{10.7} = 74$, $F_{\mathrm{bg}} = 67$), when the F74113 reference spectrum was measured, and solar maximum conditions with $F_{10.7} = 200$, $F_{\mathrm{bg}} = 100$ corresponding to the EUVAC model for $P = 200$ are compared in Table 1. Parameter $P = (FA_{10.7} + F_{10.7})/2$ is used as the proxy in the EUVAC model [*Richards et al.,* 1994], $FA_{10.7}$ being an 81-day average of the daily $F_{10.7}$ index.

Our usual model calculations (a standard mode) are based on the photoionization and photoabsorption cross sections mostly from *Torr et al.* [1979]. Photoionization cross section for $\mathrm{O}^+(^4S)$, $\mathrm{O}^+(^2P)$, and $\mathrm{O}^+(^2D)$ production were taken according to *Richards and Torr* [1988], with allowance for the secondary ionization for $\lambda < 250$ Å according to *Ivanov-Kholodny and Nikol'sky* [1969]. Their approach is based on the experimental fact that each act of ionization by short-wave UV or X-ray emission requires ε amount of energy. This $\varepsilon = 32$ eV for the emission with $\lambda \leq 200$ Å. Then the effective ionization cross section is defined as

$$\sigma_i = \sigma_{iph} E/\varepsilon = 387 \sigma_{iph} \lambda^{-1} \tag{1}$$

where E is the energy of the initial photon, and σ_{iph} is the photoionization cross section, and λ is the wavelength in Å. For the sake of comparison, the same calculations were performed with the cross sections given by *Fennely and Torr* [1992], taking into account secondary ionization for $\lambda < 400$ Å, as proposed by *Titheridge* [1996].

The list of chemical reactions used in the model is given in Table 2. Reaction rates were taken from *Buonsanto et al.* [1992], *McEwan and Phillips* [1975], *Oppenheimer et al.* [1977], *Torr and Torr* [1979], and *McFarland et al.* [1973].

Neutral composition (O, O_2, N_2, N) and temperature T_n

Table 2. Chemical Reactions Used in the Model

Reaction	Rate coefficient, cm^{-3} s^{-1}, or rate, s^{-1}
$O^+(^4S) + N_2 \rightarrow NO^+ + N$	$1.2 \times 10^{-12}(300/T_{eff})$ $T_{eff} < 740$ K $8.0 \times 10^{-14}(300/T_{eff})^{-2}$ $T_{eff} > 740$ K
$O^+(^4S) + O_2 \rightarrow O_2^+ + O$	$1.0 \times 10^{-9}/T_n^{0.7}$
$O^+(^4S) + NO \rightarrow NO^+ + O$	8.0×10^{-13}
$O^+(^2D) + O \rightarrow O^+(^4S) + O$	1.0×10^{-10}
$O^+(^2D) + N_2 \rightarrow N_2^+ + O$	1.0×10^{-9}
$O^+(^2D) + O_2 \rightarrow O_2^+(a^4\Pi) + O$	8.0×10^{-10}
$O^+(^2D) + e \rightarrow O^+(^4S) + e$	$6.6 \times 10^{-8}(300/T_e)^{0.5}$
$O^+(^2P) + O \rightarrow O^+(^4S) + O$	1.8×10^{-10}
$O^+(^2P) + N_2 \rightarrow N_2^+ + O$	5.0×10^{-11}
$O^+(^2P) + N_2 \rightarrow O^+(^4S) + N_2$	4.0×10^{-10}
$O^+(^2P) + e \rightarrow O^+(^2D) + e$	$1.5 \times 10^{-7}(300/T_e)^{0.5}$
$O^+(^2P) + e \rightarrow O^+(^4S) + e$	$3.2 \times 10^{-8}(300/T_e)^{0.5}$
$O^+(^2P) \rightarrow O^+(^2D) + h\nu$	$A = 0.173$ s^{-1}
$O^+(^2P) \rightarrow O^+(^4S) + h\nu$	$A = 0.048$ s^{-1}
$O_2^+(X^2\Pi) + N \rightarrow NO^+ + O$	1.8×10^{-10}
$O_2^+(X^2\Pi) + N \rightarrow N^+ + O_2$	4.0×10^{-10}
$O_2^+(X^2\Pi) + N_2 \rightarrow NO^+ + NO$	1.0×10^{-15}
$O_2^+(X^2\Pi) + NO \rightarrow NO^+ + O_2$	4.4×10^{-10}
$O_2^+(X^2\Pi) + e \rightarrow O + O$	$1.95 \times 10^{-7}(300/T_e)^{0.7}$
$N_2^+ + O \rightarrow O^+(^4S) + N_2$	$1.0 \times 10^{-11}(300/T_n)^{0.23}$
$N_2^+ + O \rightarrow NO^+ + N$	$1.4 \times 10^{-10}(300/T_n)^{0.44}$ ($\times 1.3$)
$N_2^+ + O_2 \rightarrow O_2^+ + N_2$	$5.0 \times 10^{-11}(300/T_n)$
$N_2^+ + NO \rightarrow NO^+ + N_2$	4.8×10^{-10}
$N_2^+ + N \rightarrow N^+ + N_2$	1.0×10^{-11}
$N_2^+ + e \rightarrow N + N$	$3.5 \times 10^{-7}(300/T_e)^{0.5}$
$N^+ + O_2 \rightarrow O^+(^4S) + NO$	3.6×10^{-11}
$N^+ + O_2 \rightarrow NO^+ + O$	2.6×10^{-10}
$N^+ + NO \rightarrow NO^+ + N$	2.0×10^{-11}
$N^+ + O_2 \rightarrow O_2^+ + N$	3.1×10^{-10}
$N^+ + O \rightarrow O^+(^4S) + N$	2.2×10^{-12}
$NO^+ + e \rightarrow N + O$	$4.5 \times 10^{-7}(300/T_e)^{0.83}$

were used from the MSIS 86 thermospheric model [*Hedin,* 1987]. Nitric oxide, NO, is very important for E-layer chemistry. It was found by fitting the calculated NO^+/N_e and O_2^+/N_e ratios in the 100–120 km height range to the ion composition model by *Danilov and Smirnova* [1995], which is based on rocket measurements. An effective scale height of the [NO] height distribution inferred at 115 km was used to extrapolate the [NO] profile above 120 km.

The Millstone Hill daytime observations for three winter — days 5 February 1992, 10 November 1988, and 15 January 1985 — as they are given in *Buonsanto et al.* [1995], were compared with our model calculations. These days represent quiet time E region for solar minimum (15 January 1985, $F_S = 74.7$), middle (10 November 1988, $F_S = 175.3$), and high solar activity (5 February 1992, $F_S = 207$) conditions, F_S being a three-month average of $F_{10.7}$.

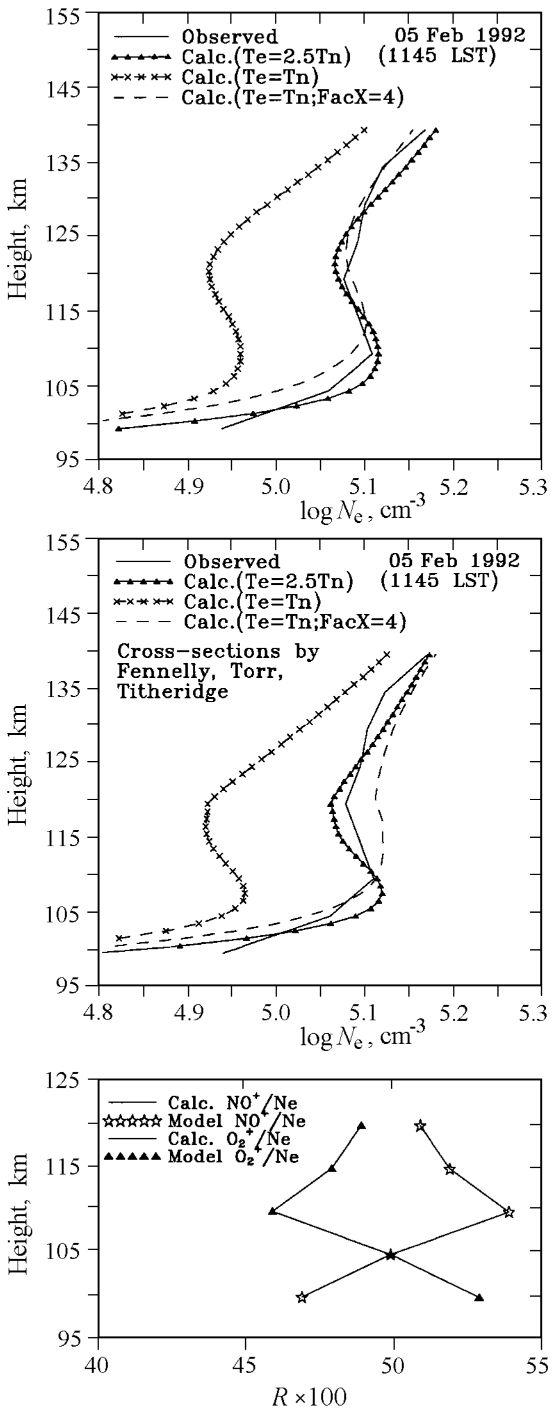

Figure 1. Electron density profiles at Millstone Hill for 1145 LST on 5 February 1992 at high ($F_S = 207$) solar activity. The observed profile is shown together with the profiles calculated using the standard set of cross sections (top panel) and with the Fennelly, Torr, and Titheridge sections (middle panel). The relative ion composition by Danilov and Smirnova fit in our model calculations is given in the bottom.

3. Calculations

Three types of model calculations were performed for two sets (see above) of photoionization and photoabsorption cross sections: (i) with standard EUV fluxes from Nusinov model and $T_e = T_n$ in the E region; (ii) with fluxes increased by four times in the 50–100 Å wavelength bin and $T_e = T_n$, and (iii) with standard model fluxes, but $T_e = 2.5T_n$ in the E-layer peak around 110 km. An increase of T_e over T_n with $T_e/T_n = 3-5$ is observed in the probe measurements in the daytime E region [*Duhau and Azpiazu,* 1985]. As the dissociative recombination rate coefficients for NO^+ and O_2^+ ions depend on T_e, this effect may be important. In accordance with *Duhau and Azpiazu* [1985], a gaussian-type dependence was used to specify the T_e/T_n height distribution with the peak at 110 km. Calculations and the Millstone Hill observations are shown in Figure 1 for high solar activity (5 February 1992). The standard calculations give N_mE by lower 40% than the observed one similar to FLIP (around a 50% deficiency) and Millstone Hill photochemical model results [*Buonsanto et al.,* 1995]. The 50–100 Å flux increased by a factor of 4 does provide the observed N_mE, although h_mE is shifted to higher altitudes. Close results, but with a more realistic h_mE, may be obtained with the standard EUV model fluxes and $T_e/T_n = 2.5$ at 110 km.

Calculations with cross sections by *Fennelly and Torr* [1992] and *Titheridge* [1996] (Figure 1, middle panel) give the results that are very close to our standard model calculations (Figure 1, top), although our approach of taking into account the secondary ionization effects according to *Ivanov-Kholodny and Nikol'sky* [1969] is much simpler than the *Titheridge* [1996] approach. The 50–100 Å flux increased by four times shifts h_mE to higher altitudes as in Figure 1 (top), and the valley is not developed in this case. Contrary, the $N_e(h)$ profile calculated with $T_e/T_n = 2.5$ demonstrates a well pronounced valley.

Relative ion composition (the NO^+/N_e and O_2^+/N_e ratios) fitted to the *Danilov and Smirnova* [1995] model by varying [NO] are shown in Figure 1 (bottom). It is interesting to note that [NO^+] is higher than [O_2^+] above 105 km, but the ratio is inverse at lower heights. This crossing point shifts to lower heights as the solar activity declines (see Figures 2–3). The reason for such variations is out of the scope of this paper, but the corresponding [NO] height profiles are discussed below.

Similar results are obtained for moderate solar activity (Figure 2). Although a factor of 4 for the 50–100 Å flux provides the observed N_e around 110 km, the $N_e(h)$ profile is uplifted as a whole and the valley is not well developed with the Fennelly, Torr, and Titheridge cross sections (Figure 2, middle panel). Calculations with $T_e/T_n = 2.5$ look more realistic with both sets of cross sections (Figure 2, top and middle boxes). The [NO^+] ions dominate over [O_2^+] in the 100–120 km height range in agreement with the Danilov and Smirnova model.

General conclusions concerning the results for solar minimum (Figure 3) are the same as above. The only difference is that a factor of 4 for the 50–100 Å flux is not sufficient to get the observed N_e around 110 km, while a factor of 2.5

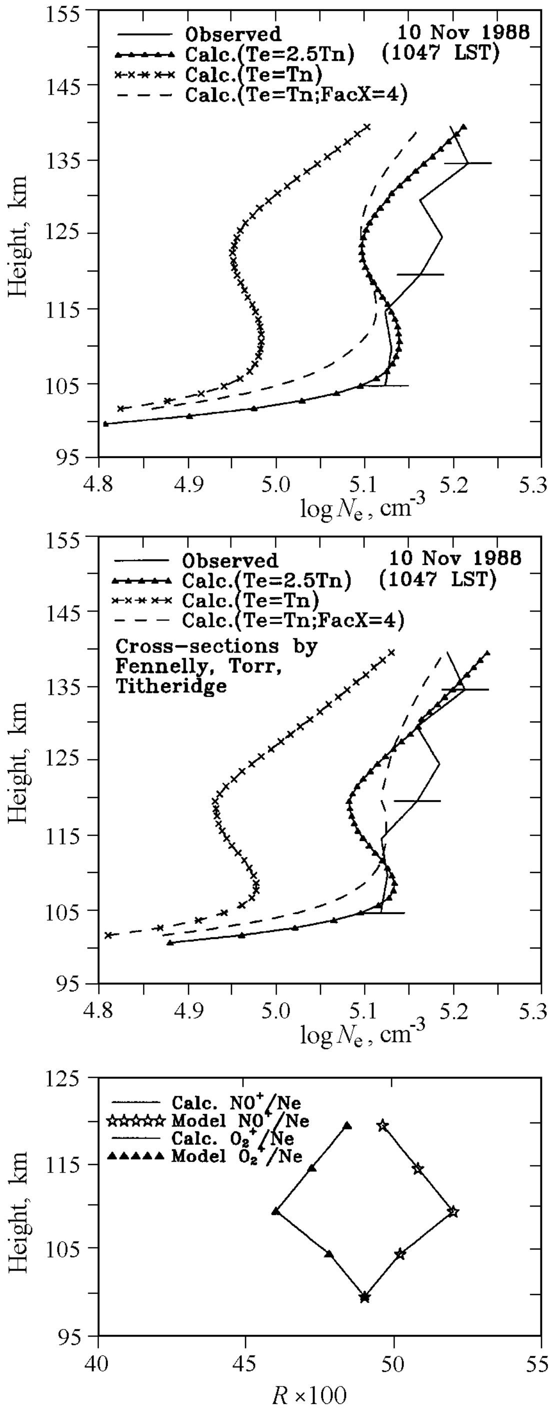

Figure 2. Same as Figure 1, but for 1047 LST on 10 November 1988 at moderate ($F_S = 175.3$) solar activity.

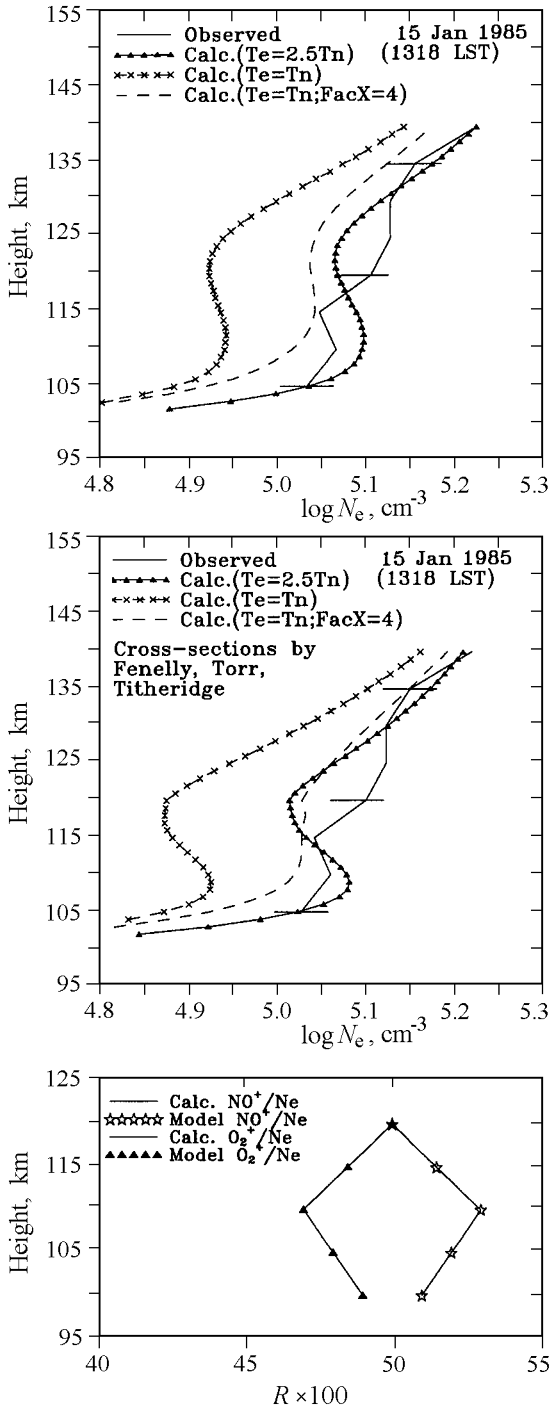

Figure 3. Same as Figure 1, but for 1318 LST on 15 January 1985 at low ($F_S = 74.7$) solar activity.

for T_e/T_n may be too high and should be decreased. Such a decrease of T_e/T_n ratio does take place at low solar activity [*Duhau and Azpiazu*, 1985]. It should be stressed that the *Danilov and Smirnova* [1995] model does not show any relative ion composition variations around 110 km (cf. Figures 1–3, bottom panels) in the course of solar cycle (around 55% for NO^+/N_e and 45% for O_2^+/N_e). This implies corresponding small [NO] variations with solar activity in the E-layer maximum (see below).

The other possibility for decreasing the NO^+ ion recombination rate and solving the problem of low calculated N_mE is to use the low dissociative recombination rate coefficient $\alpha(NO^+) = 2.3 \times 10^{-7}(300/T_e)^{0.5}$ of *Mul and McGowan* [1979]. Calculations with this rate coefficient provide the

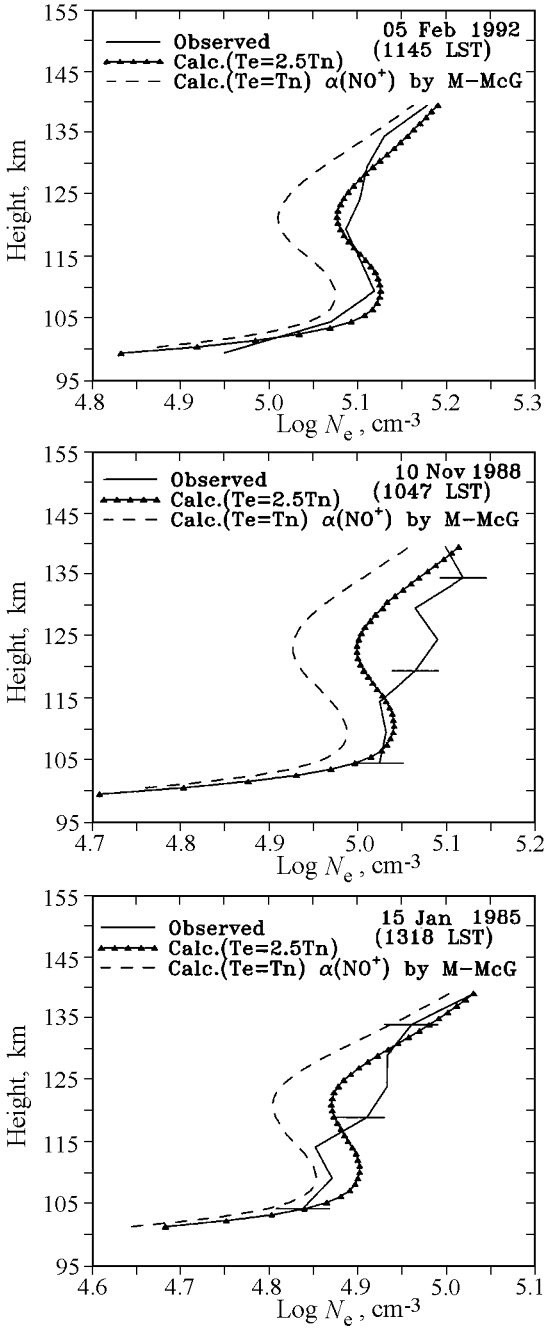

Figure 4. Observed and calculated with $\alpha(NO^+)$ by Mul and McGowan and $T_e/T_n = 1.5$ (dashes) electron density profiles for three days considered. Calculations with a conventional value of $\alpha(NO^+) = 4.5 \times 10^{-7}(300/T_e)0.83$ and $T_e/T_n = 2.5$ are given for a comparison. The Nusinov EUV model with $F_{ac}X = 1$ and standard cross-sections are used in calculations. M-McG refers to the Mul and McGowan $\alpha(NO^+)$.

observed N_e around 110 km with $T_e = 1.5T_n$ and the standard model of 50–100 Å fluxes. The results are very close to those obtained with $\alpha(NO^+) = 4.5 \times 10^{-7}(300/Te)^{0.83}$, $T_e/T_n = 2.5$ at 110 km. Both curves are given for a comparison in Figure 4 for three days considered. A well defined h_mE at 107–110 km and a valley at 120–125 km may be obtained in this case. The standard set of cross sections was used in these calculations.

Each set of calculations was performed with [NO] fitted to provide the *Danilov and Smirnova* [1995] model NO^+/N_e and O_2^+/N_e values in the 100–120 km height range. Above 120 km [NO] was extrapolated with an effective scale height found at 115 km. The calculated [NO] distributions are given in Figure 5 for three days in question. Only calculations that provide N_e at 110 km close to the incoherent scatter (IS) observations are shown in Figure 5. The calculated [NO] height variation is seen to be a Chapman type layer with a peak around 107 km and a scale height of 10 ± 2 km. A dependence of $[NO]_{max}$ on solar activity is seen with $[NO]_{max}$ on 5 February 1992 being higher than on 15 January 1985.

4. Discussion

There are two ways to overcome the problem with low calculated N_mE: either to increase the photoionization rate in the E-layer peak or to reduce the recombination rate of NO^+, which is the major ion in the E region.

Let us consider the first possibility. For the classic daytime Chapman E layer, the photoionization rate in its peak may be written as

$$q_{\max} = \frac{I_\infty}{H} \frac{\sigma_i}{\sigma_a} \frac{\cos \chi}{e} \tag{2}$$

To increase $q_{\max}$, one may increase I_∞ (the ionization flux) or decrease H (the scale height of the ionized atmospheric neutral species). In their earlier monograph *Ivanov-Kholodny and Nusinov* [1979] proposed considering strong seasonal variations of molecular oxygen scale height in the E region with small winter $H(O_2)$ values. Along with this they used low $\alpha(NO^+)$ by *Mul and McGowan* [1979]. This approach allowed them to explain many morphological features of the E layer. Unfortunately low winter $H(O_2)$ results in lower winter h_mE as compared to the summer one. On one hand, this contradicts the incoherent scatter observations made in Kharkov (49.43°N, 36.92°E) and presented in the monograph by *Antonova et al.* [1996], where winter h_mE values are higher than summer ones. On the other hand, according to MSIS 86 thermospheric model [*Hedin*, 1987], the concentration of the major neutral (O_2, N_2, O) species is higher in winter at the midlatitude E region, and this should result in higher winter h_mE values.

The other possibility is to increase I_∞ in (2). The ionization rate should be doubled at the E-layer peak if the *Nusinov* [1992] EUV model is used (Figures 1–3, $T_e = T_n$). This cannot be done for two UV lines with $\lambda = 977$ Å (CIII) and 1026 Å (Lyman-β), producing the main ionization in the E region as the present day accuracy of measurements in the UV range of spectrum is high enough [*Woods et al.,* 1998]. On the other hand there is large uncertainty with EUV fluxes for $\lambda < 150$ Å. Initial fluxes have been tripled for the $\lambda = 50 - 150$ Å interval in the EUVAC model [*Richards et al.,* 1994], but an additional increase up to a factor of 4 is required to get the experimental N_mE values [*Titheridge*, 1997]. The same increase of the fluxes with $\lambda = 50 - 100$ Å by a factor of 4 is needed for the Nusinov model to obtain the observed N_mE (Figures 1–3). Such an increase of the soft X-ray radiation changes (in favor of X rays) the proportion between UV and X-ray contributions to the E-layer ionization rate. According to *Titheridge* [1997], about 66% of the E-region ionization is produced by radiation with $\lambda < 150$ Å. The X-ray contribution will be even larger if one uses the required factor of 4 for this wavelength interval in the EUVAC model. In case of the Nusinov EUV model, such an increase by a factor of 4 would give a 55% X-ray contribution to the total ionization rate at 110 km. It is possible to show that such an increase of the X ray contribution to the E-layer ionization rate leads to a contradiction with ionospheric observations.

One of the ways to estimate the X-ray contribution to the E-layer total ionization rate is to analyze N_mE variations during solar flares [*Ivanov-Kholodny et al.,* 1976, 1977]. According to rocket and satellite observations, a strong increase of the X-ray emission takes place in 1–8, 8–20, and 44–60-Å spectrum intervals during solar flares while only small changes of the UV radiation were observed [*Chubb et al.,* 1957]. Therefore, we may suppose for our estimates that the UV ionization rate does not change during solar flares. The I_x flux in the 8–165 Å spectrum range, which ionizes the E region, is related to the 8–20 Å flux as $I_x \propto (I_{8-20})^{0.5}$ [*Ivanov-Kholodny et al.,* 1976]. Regular observations of X-ray emission in the ionization chambers on board satellites are available and published in Solar Geophysical Data. For strong flares analyzed by *Ivanov-Kholodny et al.* [1977], the I_{8-20} emission measured on board the SOLRAD 9 and 10 satellites increased by five to 25 times. Therefore, for our estimates we may take an average factor of 3.6 for the I_x increase during the flare events considered. Then the proposed increase by a factor of 4 of the X-ray emission with a 55–66% (mean 60%) X-ray contribution to the total E-layer ionization rate results in

$$q_f = 0.4q_0 + 0.6q_0 F_{ac} I_x \qquad (3)$$

where q_0 and q_f are the total E-layer ionization rate for quiet and flare conditions, respectively, and $F_{ac}I_x = 3.6$ is an average X-ray emission increase. Therefore, we get $q_f = 2.56q_0$. On the other hand, the observed N_mE variations for the flares considered [*Ivanov-Kholodny et al.,* 1977] give, on the average, $q_f = (1.44 - 1.60)q_0$ with a lower value for winter and a larger one for summer periods. This is much less than a factor of 2.56 obtained for the fourfold increase in X-ray emission required to get the observed N_mE in model calculations. Thus this proposal should be ruled out. The observed $q_f = (1.44 - 1.60)q_0$ implies only a 17–23% X-ray contribution to the total E-region ionization rate. X-ray relative contribution of 18% was obtained by *Ivanov-Kholodny and Nusinov* [1979] for moderate solar activity. The EUV model by Nusinov provides the required X-ray relative contribution while the EUVAC model strongly overestimates it (see Table 1 for the 50–100 Å bin) not to mention an additional increase of the flux in this wavelength bin proposed by *Titheridge* [1997]. Therefore, there is no way to solve the problem of low calculated N_mE by a photoionization rate increase. It should be mentioned that according to recent soft X-ray measurements (20–100 Å) on board the Student

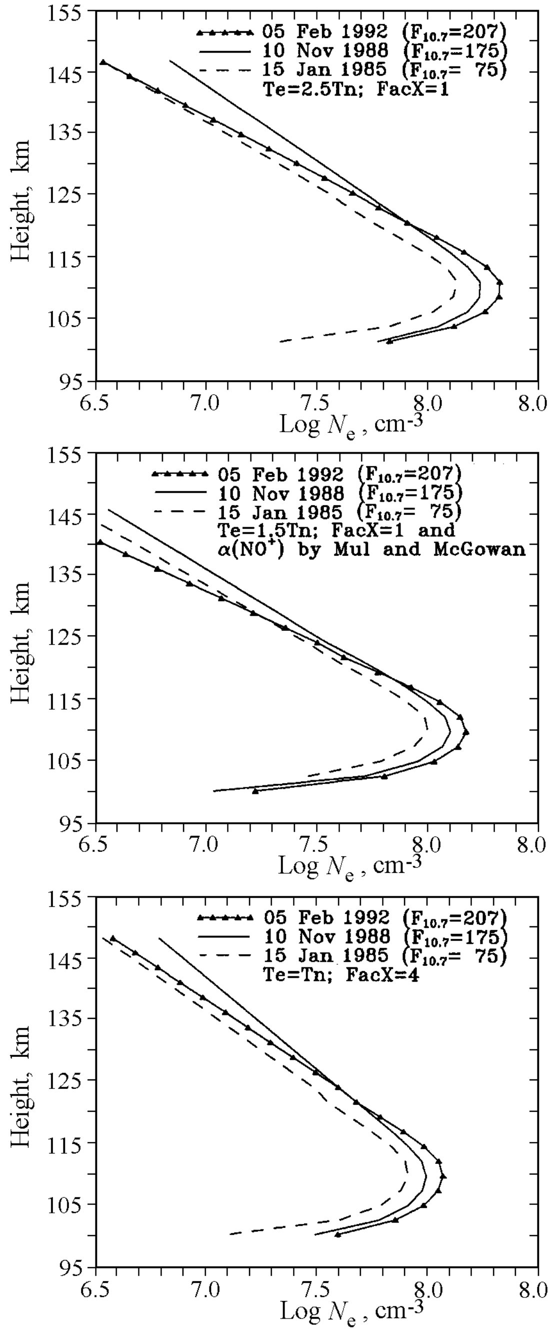

Figure 5. Calculated NO profiles for three days in question and other conditions given in the legend. M-McG refers to the Mul and McGowan $\alpha(NO^+)$ used in the calculations.

Nitric Oxide Explorer (SNOE) satellite [*Bailey et al.,* 1999], the extrapolation of the measured irradiance to the solar minimum gives much lower values than the EUVAC predictions.

Let us consider the other possibility — a decrease of $\alpha(\mathrm{NO}^+)$. The N_mE observations can be well reproduced in our calculations if $T_e > T_n$ is accepted in the daytime E region in agreement with the probe measurements [*Duhau and Azpiazu*, 1985]. A moderate $T_e/T_n = 2.5$ ratio is required at the E-layer peak (around 110 km) with a conventional $\alpha(\mathrm{NO}^+) = 4.5 \times 10^{-7}(300/T_e)^{0.83}$ to obtain the observed N_mE (Figures 1–3). The required T_e/T_n ratio may be even 1.5 if a small $\alpha(\mathrm{NO}^+) = 2.3 \times 10^{-7}(300/T_e)^{0.5}$ rate coefficient given by *Mul and McGowan* [1979] is used (Figure 4). Unlike *Duhau and Azpiazu* [1985], who found strong dependence of T_e/T_n ratio on solar activity, practically an unchanged T_e/T_n is required in our calculations at all levels of solar activity. Physical mechanism of such T_e heating at middle latitudes is not clear yet [*Duhau and Azpiazu*, 1985]. It should be mentioned that no difference between T_e and T_i (which coincides with T_n in the midlatitude E region) is observed by the incoherent scatter method at middle latitudes. Such T_e enhancement over T_i due to the relative electron-ion drift takes place in the auroral zone, according to the EISCAT observations [*Igarashi and Schlegel*, 1987]. Nevertheless, a possibility of T_e being higher T_n seems very promising in solving the problem of low calculated q/α_{eff} for the daytime E layer.

Our calculations (Figures 1–3, top panels) reproduce a reasonable depth of the $E-F1$ valley. According to the IRI 90 model [*Bilitza*, 1990], the valley depth (N_{val}/N_mE) is 10–12% for the conditions in question. The valley depth of 13–15% is given by the empirical models [*Chasovitin et al.,* 1983; *Fatkullin et al.,* 1981]. Kharkov incoherent scatter observations [*Tkachev*, 1981] give the depth of the noon valley as 12–18%. The calculated $N_e(h)$ profiles (Figures 1–3, top panels, $T_e = 2.5T_n$) have the valley depth of 10–15%. The profiles calculated with $F_{ac}X = 4$ for the 50–100 Å wavelength interval show an undeveloped valley. Normal valley with a depth of 10–13% is provided by the *Mul and McGowan* [1979, (Figure 4)] calculations with $T_e = 1.5T_n$, $F_{ac}X = 1$, and $\alpha(\mathrm{NO}^+)$. Close results are obtained with the *Fennelly and Torr* [1992] and *Titheridge* [1996] cross sections (Figures 1–3, middle panels). Therefore, a proper EUV spectrum is more important for development of a normal valley than different sets of cross sections used in calculations.

Problems with calculated $\mathrm{NO}^+/\mathrm{O}_2^+$ ratio [*Buonsanto et al.,* 1995; *Titheridge*, 1997], which contradicts rocket measurements in the E region, mostly is related with a correct specification of the [NO] distribution. In our approach we make a self-consistent [NO] fitting to get NO^+/N_e and O_2^+/N_e ratios as in the *Danilov and Smirnova* [1995] model, which is based on rocket observations. The calculated [NO] profiles (Figure 5) demonstrate small variations with solar activity, the [NO] peak density at 107 km being larger only by 40% at high solar activity. This is much less than solar cycle variations (4–5 times for winter) used by *Titheridge* [1997] in his analysis. The other difference is in the NO peak density which is lower in his model by 10–2.5 times when we pass from low to high solar activity. On the other hand, a theoretical model by *Gerard et al.* [1997] gives the NO peak values, which are much closer to our results. Close NO values were observed by SNOE satellite at geomagnetic latitudes of Millstone Hill for a quiet ($Ap = 12$) day following a period of moderate disturbance with $Ap = 28$ [*Solomon et al.,* 1999]. However, it should be stressed that the obtained [NO] solar cycle variation is an estimate based on the model [*Danilov and Smirnova*, 1995] ion composition, which demonstrates very small solar activity variation in the E region.

The effective scale height inferred at 115 km from the calculated [NO] distribution is about 8–12 km, depending on the calculation mode. This is close to $H(\mathrm{NO}) = 8-9$ km used by *Titheridge* [1997, and references therein], but unlike his dependence on solar activity there is a tendency for $H(\mathrm{NO})$ to be less at solar maximum (Figure 5, top and middle panels). Similar dependence of $H(\mathrm{NO})$ at 120 km on solar activity may be found in *Gerard et al.* [1997].

5. Conclusions

The main results of our analysis are the following:

1. The observed at Millstone Hill daytime N_mE may be reproduced in model calculations provided that the 50–100 Å flux is increased by a factor of 4 in the *Nusinov* [1992] EUV model. The same increase is required in case of the EUVAC model as was proposed by *Titheridge* [1997]. But such an increase distorts the proportion between UV and X-ray contributions in favor of X ray (around 60%) to the total photoionization rate in the E region. This leads to a contradiction with N_mE observations during solar flares. As was shown by *Ivanov-Kholodny and Nusinov* [1979], the X-ray contribution to the E-layer total ionization rate for quiet conditions is around 20%, depending on solar activity; our analysis gives a similar estimate. The EUV model by *Nusinov* [1992] provides this contribution while the EUVAC model (where the 50–150 Å flux was tripled) does not. Therefore, a proposal to obtain the observed N_mE values in model calculations through an X-ray emission increase should be ruled out.

2. The other way to obtain the observed N_mE is to reduce $\alpha(\mathrm{NO}^+)$. One of the ways to do this is to take into account $T_e > T_n$ in the E region as it follows from the probe measurements [*Duhau and Azpiazu,* 1985]. A moderate $T_e/T_n = 2.5$ ratio at the E-layer peak (around 110 km) along with a conventional $\alpha(\mathrm{NO}^+)$ and the Nusinov EUV model is required to get the observed daytime N_mE values at different levels of solar activity. The same results may be obtained with even lower $T_e/T_n = 1.5$ ratio and $\alpha(\mathrm{NO}^+)$ by *Mul and McGowan* [1979]. Both calculations reproduce a reasonable depth of the $E-F1$ valley with $N_{\mathrm{val}}/N_mE = 10-15\%$ close to the empirical ionospheric models. But the reality of $T_e > T_n$ in the midlatitude daytime E region is questionable because the probe results are not confirmed by incoherent scatter observations.

3. The E-layer ion composition with $[\mathrm{NO}^+] > [\mathrm{O}_2^+]$ corresponding to the rocket observations can be reproduced in model calculations using an appropriate [NO] height distribution. These [NO] profiles may be obtained by fitting the

calculated ion composition in the 100–120 km height range to the model based on rocket measurements. The calculated [NO] is a Chapman type layer with a peak around 107 km and a scale height of 8–12 km inferred at 115 km. The [NO] peak density varies with solar activity being larger by 40% at $F_{10.7} = 207$ compared to solar minimum ($F_{10.7} = 75$) conditions. The obtained [NO] solar cycle variation should be considered as an estimate based on model [*Danilov and Smirnova*, 1995] ion composition variations; the latter show no solar activity variation at the E-layer maximum around 110 km.

Acknowledgments. This work was in part supported by the Russian Foundation for Basic Research under Grant 98-05-64191.

References

Antonova, L. A., G. S. Ivanov-Kholodny, and V. E. Chertoprud, *Aeronomy of E layer (in Russian),* Janus, Moscow, 1996.

Bailey, S. M., T. N. Woods, C. A. Barth, and S. C. Solomon, Measurements of the solar soft X ray irradiance from the Student Nitric Oxide Explorer, *Geophys. Res. Lett., 26*, 1255, 1999.

Bilitza, D., (ed.), International Reference Ionosphere IRI 90, URSI-COSPAR, *Rep. NSSDC/WDC A Rocket and Satellites*, Greenbelt, Maryland, 1990.

Bruevich, E. A., and A. A. Nusinov, The spectrum of the short-wave radiation for aeronomical calculations under various levels of solar activity, *Geomagn. Aeron., 24 (in Russian),* 581, 1984.

Buonsanto, M. J., S. C. Solomon, and W. K. Tobiska, Comparison of measured and modeled solar EUV flux and its effect on the $E - F1$ region ionosphere, *J. Geophys. Res., 97*, 10,513, 1992.

Buonsanto, M. J., P. G. Richards, W. K. Tobiska, S. C. Solomon, Y.-K. Tung, and J. A. Fennelly, Ionospheric electron densities calculated using different EUV flux models and cross sections: Comparison with radar data, *J. Geophys. Res., 100*, 14,569, 1995.

Chasovitin, Yu. K., V. B. Shushkova, E. N. Sykilinda, and V. V. Maksimova, Empirical model of the electron concentration for low and middle latitudes at altitudes of 80–200 km, *Proc. Experim. Meteorol. Inst. (in Russian), 13*(102), 59, 1983.

Chubb, T. A., R. W. Kreplin, and H. Friedman, Rocket observation of X ray emission in a solar flare, *J. Geophys. Res., 62*, 89, 1957.

Danilov, A. D., Ion chemistry of the lower thermosphere, *J. Atmos. Terr. Phys., 56,* 1213, 1994.

Danilov, A. D., and V. K. Semenov, Relative ion composition model at midlatitudes, *J. Atmos. Terr. Phys., 40*, 1093, 1978.

Danilov, A. D., and N. V. Smirnova, Improving the 75 to 300 km ion composition model of the IRI, *Adv. Space Res., 15*(2), 171, 1995.

Duhau, S., and C. M. Azpiazu, Empirical model of the E region electron temperature around noon and at low magnetic activity, *Planet. Space Sci., 33,* 909, 1985.

Fatkullin, M. N., T. I. Zelenova, V. K. Kozlov, A. D. Legenjka, and T. H. Soboleva, *Empirical Models of the Midlatitude Ionosphere*, 256 pp., Nauka, Moscow, 1981.

Fennelly, J. A., and D. G. Torr, Photoionization and photoabsorption cross sections of O, N_2, O_2, and N for aeronomic calculations, *Atmos. Data Nucl. Data Tables, 51,* 321, 1992.

Gerard, J.-C., D. V. Bisikalo, V. I. Shematovich, and J. W. Duff, An updated model of the hot nitrogen atom kinetics and thermospheric nitric oxide, *J. Geophys. Res., 102*, 285, 1997.

Hedin, A. E., MSIS 86 thermospheric model, *J. Geophys. Res., 92*, 4649, 1987.

Igarashi, K., and K. Schlegel, Electron temperature enhancement in the polar E region measured with EISCAT, *J. Atmos. Terr. Phys., 49*, 273, 1987.

Ivanov-Kholodny, G. S., and G. M. Nikol'sky, *The Sun and the Ionosphere (in Russian),* 217 pp., Nauka, Moscow, 1969.

Ivanov-Kholodny, G. S., and A. A. Nusinov, Formation and dynamics on the daytime midlatitude ionospheric E layer, *Proc. Inst. Appl. Geophys. (in Russian), 37*, 1979.

Ivanov-Kholodny, G. S., L. N. Letshenko, and I. N. Odintzova, Relationship between X ray and ultraviolet radiations of solar flares in the ionization of the ionosphere E region, *Geomagn. Aeron. (in Russian), 16*, 246, 1976.

Ivanov-Kholodny, G. S., L. N. Letshenko, A. A. Nusinov, and I. N. Odintzova, Influence of seasonal variations of neutral atmosphere on ionization of the ionospheric E region, *Geomagn. Aeron. (in Russian), 17*, 839, 1977.

Katjushina, V. V., M. V. Krasinets, A. A. Nusinov, Ch. A. Bart, and G. J. Rottman, A two-component model of the $Ly\alpha$ emission depending on solar activity level, *Geomagn. Aeron. (in Russian), 31*, 40, 1991.

McEwan, M. J., and L. F. Phillips, *Chemistry of the Atmosphere*, Edward Arnold, London, 1975.

McFarland, M., D. L. Albritton, F. C. Fehsenfeld, E. E. Ferguson, and A. L. Schmeltekopf, Flow-drift technique for ion mobility and ion-molecular reaction rate constant measurements, II. Positive ion reactions of N^+, O^+, and N_2^+ with O_2 and O^+ with N_2 from thermal to 2 eV, *J. Chem. Phys., 59*, 6620, 1973.

Mul, P. M., and J. W. McGowan, Temperature dependence of dissociative recombination for atmospheric ions NO^+, O_2^+ and N_2^+, *J. Phys., B12*, 1591, 1979.

Nusinov, A. A., A dependence of intensity of EUV lines on solar activity level, *Geomagn. Aeron. (in Russian), 24*, 529, 1984.

Nusinov, A. A., Models for prediction of EUV and X ray solar radiation based on 10.7-cm radio emission, *Proc. Workshop on Solar Electromagnetic Radiation for Solar Cycle 22, Boulder, Colo., July 1992*, edited by R. F. Donnely, NOAA ERL, Boulder, Colo., USA, 354, 1992.

Nusinov, A. A., L. A. Antonova, and V. V. Katushina, Solar fluxes in the 10- to 30-nm range according to studies of the E region and the interlayer ionization valley, *Int. J. Geomagn. Aeron., 1*, 153, 1999.

Oppenheimer, M., E. R. Constantinides, K. Kirby-Docken, G. A. Victor, A. Dalgarno, and J. H. Hoffman, Ion photochemistry of the thermosphere from Atmosphere Explorer C measurements, *J. Geophys. Res., 82*, 5485, 1977.

Richards, P. G., and D. G. Torr, Ratios of photoelectron to EUV ionization rates for aeronomic studies, *J. Geophys. Res., 93*, 4060, 1988.

Richards, P. G., J. A. Fennelly, and D. G. Torr, EUVAC: A solar EUV flux model for aeronomic calculations, *J. Geophys. Res., 99*, 8981, 1994.

Solomon, S. C., C. A. Barth, and S. M. Bailey, Auroral production of nitric oxide measured by the SNOE satellite, *Geophys. Res. Lett., 26*, 1259, 1999.

Titheridge, J. E., Direct allowance for effect of photoelectrons in ionospheric modeling, *J. Geophys. Res., 101*, 357, 1996.

Titheridge, J. E., Model results for the ionospheric E region: Solar and seasonal changes, *Ann. Geophys., 15*, 63, 1997.

Tkachev, G. N., About the depth of the valley between layers E and F of the ionosphere, *Geomagn. Aeron. (in Russian), 21*, 939, 1981.

Torr, M. R., D. G. Torr, R. A. Ong, and H. E. Hinteregger, Ionization frequencies for major thermospheric constituents as a function of solar cycle 21, *Geophys. Res. Lett., 6*, 771, 1979.

Woods, T. N., G. J. Rottman, S. M. Bailey, S. C. Solomon, and J. R. Worden, Solar extreme ultraviolet irradiance measurements during solar cycle 22, in *Solar Electromagnetic Radiation Study for Solar Cycle 22*, Kluwer I.R. Academic Publ., Dordrecht, 133, 1998.

A. V. Mikhailov, Institute of Terrestrial Magnetism, Ionosphere and Radio Wave Propagation, Troitsk 142092, Moscow Region, Russia. (avm71@orc.ru)

(Received 22 February 2000; accepted 6 January 2003)